Chapter 3

A peptide core motif for binding heterotrimeric G protein α subunits

William W. Ja and Richard W. Roberts

Recently, *in vitro* selection using mRNA display was used to identify a novel peptide sequence that binds with high affinity to $G_{i\alpha1}$. The peptide was minimized to a 9-residue sequence (R6A-1) that retains high affinity and specificity for the GDP-bound state of $G_{i\alpha1}$ and acts as a guanine nucleotide dissociation inhibitor (GDI). Binding assays with immobilized R6A-1 reveal that the peptide interacts with G_{α} subunits representing all four G protein classes [i1–3, oA, q, s(s), 12, and 15], in contrast with the consensus G protein regulatory (GPR) sequence, a 28-mer peptide GDI derived from the GoLoco/GPR motif, which binds only to $G_{i\alpha1-3}$ in this assay. Binding to R6A-1 by G_{α} subunits completely excludes association with $G_{\beta\gamma}$. These findings suggest that the R6A-1 core motif might be suitable as a starting point for the identification of peptides exhibiting novel activities and/or specificity for particular G protein subclasses. A new mRNA display library based on the R6A-1 sequence has been constructed and used to select for peptides that bind $G_{i\alpha1}$, confirming that the 9-mer core is the minimal consensus. Negligible conservation is seen in residues flanking the core motif, suggesting that they play a minimal role in binding. However, these flanking regions may confer unique properties to the core peptide and the selected peptides are currently being characterized by their binding specificities to other G proteins.

Introduction

Heterotrimeric guanine nucleotide-binding proteins (G proteins), composed of α, β, and γ subunits, mediate signaling from cell-surface receptors (GPCRs)[1] to a wide variety of effectors (*1, 2*). In the inactive state, intracellular $G_{\alpha\beta\gamma}$ heterotrimers are coupled to the membrane-spanning GPCR. Activation of the receptor results in GDP exchange with GTP in the G_α subunit, dissociation of $G_{\beta\gamma}$ heterodimers from G_α, and subsequent signal transduction through G_α-GTP and/or $G_{\beta\gamma}$. The inherent guanosine triphosphatase (GTPase) activity of G_α, which is accelerated by various GTPase-activating proteins (GAPs), returns the protein to the GDP-bound state, resulting in reassociation with $G_{\beta\gamma}$ and termination of signaling.

Approximately 50% of currently marketed drugs target GPCRs (*3, 4*). Drug discovery targeting G proteins directly has traditionally been difficult due to (1) the broad spectrum of signaling events mediated at the G protein level, (2) the requirement that drugs must cross the cell membrane to reach intracellular G proteins, and (3) the high sequence and structural similarities between G protein classes (*5, 6*). Nevertheless, a number of diseases have been attributed to aberrant G protein activity (*7, 8*) and direct G protein ligands will provide new approaches and selectivities for drug treatment (*5, 6*).

Selection methodologies can facilitate the isolation of rare molecules with unique functions, such as specificity for particular G protein classes, from large libraries (*9, 10*). We recently demonstrated that mRNA display, a selection technique where peptides are covalently attached to their encoded RNA, could be used to isolate $G_{i\alpha1}$-binding

[1] Abbreviations: GAP, GTPase-activating protein; GDI: guanine nucleotide dissociation inhibitor; GoLoco, $G_{\alpha i/o}$-Loco interaction; GPCR, G protein-coupled receptor; GPR, G protein regulatory; MALDI-TOF, matrix-assisted laser desorption/ionization time-of- flight; MBP, maltose-binding protein.

sequences (*11*). The dominant peptide from the selection, as well as a minimized, active 9-mer sequence (R6A-1), acts as a guanine nucleotide dissociation inhibitor (GDI) and competes with $G_{\beta\gamma}$ for binding to $G_{i\alpha1}$.

To examine the specificity of R6A-derived sequences, we assayed binding of various *in vitro* translated G_α subunits to immobilized peptides. Surprisingly, the R6A-1 core motif binds strongly to all tested G_α subunits. Binding of R6A-1 is generally specific for the GDP-bound state of each G_α subunit and appears to exclude heterotrimer formation with $G_{\beta\gamma}$. A new mRNA display library based on the core motif was synthesized and used to select for peptides that bind $G_{i\alpha1}$ in either the GDP or the GDP-AlF_4^- state. Functional sequences were isolated quickly (within three rounds of selection), demonstrating the utility of the library for identifying G protein-binding sequences. We are currently characterizing several of the newly isolated peptides and using the core motif library to target other G protein subclasses.

Experimental Procedures

Materials

Human cDNA clones encoding various G proteins were obtained from the UMR cDNA Resource Center (http://www.cdna.org) in the pcDNA3.1+ vector (Invitrogen Corp., Carlsbad, CA). The G_α subunits used were i1, i2, i3, oA, q, s (short-form), 12, and 15. All *in vitro* translated G_β and G_γ subunits refer to $G_{\beta1}$ and N-terminal hemagglutinin (HA) tagged $G_{\gamma2}$, respectively. Reagents were obtained from Sigma or VWR, unless otherwise noted. DNA oligos were synthesized by Integrated DNA Technologies, Inc. (Coralville, IA) except for the 115.1 library template which was synthesized at the W.M. Keck

Facility (Yale University, New Haven, CT). DNA sequencing of selected clones was performed by Laragen, Inc. (Los Angeles, CA) from purified plasmids.

Peptide/protein preparation

The C-terminal amidated peptides GPR-biotin (TMGEE DFFDL LAKSQ SKRLD DQRVD LAGQL RNSYA **K**, **K** = biocytin), L19 GPR (TMGEE DFFDL LAKSQ SKRLD DQRVD LAGYK), R6A-1-biotin (DQLYW WEYLQ LRNSY A**K**), R6A-1 (DQLYW WEYL), and R6A-4 (SQTKR LDDQL YWWEY L) were synthesized and purified as described previously (*11*). R6A-4 lacks an N-terminal methionine that the originally studied "full-length" R6A peptide contained. Peptide masses were confirmed by MALDI-TOF mass spectrometry and concentrations were determined using a calculated extinction coefficient (http://paris.chem.yale.edu/extinct.html) for absorbance at 280 nm. Biotinylated peptides were immobilized using streptavidin-agarose (Immobilized NeutrAvidin on Agarose, Pierce). Approximately 500–800 pmol of biotinylated peptide were used per 10 μL of agarose.

Full-length R6A (MSQTK RLDDQ LYWWE YL) was expressed as a fusion to maltose-binding protein (MBP) using an *in vivo* biotinylation system (*12*). Cloning, expression, and purification were performed as described previously (*11*). R6A-MBP or MBP was immobilized by random amine coupling on CNBr-sepharose 4B (Amersham Biosciences, Piscataway, NJ) as per the manufacturer's instructions at a concentration of approximately 1 mg/mL of the hydrated matrix.

N-terminal biotinylated $G_{i\alpha1}$ (Nb-$G_{i\alpha1}$) and $G_{i\alpha3}$ (Nb-$G_{i\alpha3}$) were expressed and purified as described previously (*11*). Nb-$G_{i\alpha2}$ was constructed and expressed similarly.

In vitro *translation*

All G protein subunits were translated separately in coupled transcription/translation reactions using the TNT reticulocyte lysate system (Promega, Madison, WI). Typically, 0.3–1.0 μg of plasmid DNA and 25 μCi of L-[^{35}S]-methionine (MP Biomedicals, Irvine, CA) were used in a 25 μL reaction. Translation efficiency of G_α subunits was quantitated by TCA precipitation of a 2 μL aliquot of each reaction, as per the manufacturer's instructions. G_γ reactions were supplemented with 10 μM mevalonic acid lactone to ensure complete polyisoprenylation (*13*). To make $G_{\beta\gamma}$ heterodimers, independently translated subunits were mixed together (3:1 by volume, G_β:G_γ) and incubated at 37 °C for 30 min. To reconstitute $G_{\alpha\beta\gamma}$ heterotrimers, equal volumes of G_α and preformed $G_{\beta\gamma}$ were mixed and incubated at 37 °C for an additional 30 min. For the heterotrimer immunoprecipitation assays, G_β was translated without radioactive labeling due to possible interference in the resolution of G_α subunits by SDS-PAGE. These unlabeled reactions were supplemented with L-methionine (40 μM final)

G_α interaction assay

G_α translation reactions were desalted and exchanged using MicroSpin G-25 columns (Amersham) into buffer [50 mM HEPES-KOH at pH 7.5, 6 mM $MgCl_2$, 75 mM sucrose, 1 mM EDTA, 1 μM GDP, and 0.05% (v/v) Tween 20 (Bio-Rad Laboratories, Hercules, CA)]. Equivalent aliquots (2 to 6 μL) of the desalted G_α subunits were used for the *in vitro* binding assays. G_α was added to 0.6 mL of binding buffer [25 mM HEPES-KOH at pH 7.5, 5 mM $MgCl_2$, 1 mM EDTA, 150 mM NaCl, 0.05% Tween 20, 0.05% (w/v) BSA,

1 mM β-mercaptoethanol, and 10 μM GDP] containing ~10 μL matrix with or without immobilized target. After rotating at 4 °C for 1 h, samples were briefly centrifuged and the supernatant was removed. The matrix was transferred to a 0.45 μm cellulose acetate spin filter (CoStar Spin-X, Corning, Inc., Corning, NY) and washed with 3 × 0.6 mL of binding buffer at 4 °C (1500 × g, ~40 s). The washed matrix was then removed from the spin filter for scintillation counting or analysis by SDS-PAGE. Relative binding is reported (+ standard deviation, when available) based on the bound cpm divided by the input protein counts, as determined from the TCA precipitation. Assays with aluminum fluoride were performed identically, except that the binding buffer was supplemented with 50 mM NaF and 25 μM $AlCl_3$.

$G_{\alpha\beta\gamma}$ heterotrimer immunoprecipitation

Equivalent aliquots (10 μL) of reconstituted $G_{\alpha\beta\gamma}$ heterotrimer were added to 0.6 mL of binding buffer containing ~10 μL matrix or 1 μL anti-HA mAb (Sigma, clone HA-7). After rotating at 4 °C for 1 h, ~10 μL of protein G-sepharose 4B Fast Flow was added to the mAb-containing samples. After an additional 30 min of rotating at 4 °C, immobilization matrices were washed in 0.45 μm spin filters (3 × 0.6 mL of binding buffer) as described above. A 4th wash was performed in batch, after transferring the matrices to new tubes, to prevent contamination from the spin filter membrane. The samples were resuspended in 2× SDS-loading buffer, incubated at 90 °C for 5 min, and analyzed by tricine SDS-PAGE. Gels were fixed, dried *in vacuo*, and imaged by autoradiography (Storm Phosphorimager, Amersham).

$G_{\beta\gamma}$ competition assay

Approximately 10 μL of the target matrix (~1 mg Nb-G_α i1, i2, or i3 per mL of NeutrAvidin-agarose) was incubated in 0.6 mL of binding buffer with and without various concentrations of added peptide (R6A-1, R6A, or L19 GPR) for 5 min at room temperature. Equivalent aliquots (~5 μL) of ^{35}S-methionine-labeled $G_{\beta\gamma}$ heterodimers were then added and the samples were rotated at 4 °C for 1 h. Samples were washed in spin filters as described for the G_α interaction assays (3 × 0.6 mL washes) and the amount of bound, radiolabeled protein was determined by scintillation counting of the matrices. For IC_{50} determinations, binding data were scaled relative to the bound counts in the absence of peptide competitor.

115.1 library mRNA display selection

The doped R6A-1 library was constructed by PCR amplification of oligo 115.1 [5'- AGC AGA CAG ACT AGT GTA ACC GCC $(SNN)_6$ (S13) (641) (542) (521) (521) (641) (S13) (543) (642) $(SNN)_6$ CAT TGT AAT TGT AAA TAG TAA TTG TCC C; 1 = 7:1:1:1, 2 = 1:7:1:1, 3 = 1:1:7:1, 4 = 1:1:1:7, A:C:G:T; 5 = 9:1, 6 = 1:9, C:G; N = A, C, G, or T; S = C or G (ratios have been adjusted for synthesis incorporation rates)] with primers 47T7FP (5'- GGA TTC TAA TAC GAC TCA CTA TAG GGA CAA TTA CTA TTT ACA ATT AC) and 22.9 (5'-AGC AGA CAG ACT AGT GTA ACC G). PCR (40 × 200 μL reactions) was performed with 0.1 μM 115.1 template, 1 μM primers, and 200 μM each dNTP (cycling parameters: 97 °C 2 min, 52 °C 2 min, 72 °C 4 min, followed by 4 cycles of 97 °C 2 min, 58 °C 2 min, 72 °C 4 min and a 5 min at °72 C chase cycle). Amplified DNA was phenol-extracted with Phase Lock Gel (Brinkmann Instruments) and

desalted by isopropanol precipitation. *In vitro* transcription, ligation of the mRNA to the puromycin linker (pF30P), and purification of the RNA-F30P template were performed as described previously (*11*), except that the splint oligo 23.8 (5'-TTT TTT TTT TTN AGC AGA CAG AC) was used for the ligation reaction.

RNA-peptide fusions were prepared from rabbit reticulocyte lysate, purified on oligo-dT cellulose, reverse-transcribed, and selected against immobilized Nb-$G_{i\alpha1}$ as described previously (*11*) using a modified selection buffer [25 mM HEPES-KOH at pH 7.5, 150 mM NaCl, 0.05% Tween 20, 1 mM β-mercaptoethanol, 10 μM GDP, 20 μM EDTA, 5 mM $MgCl_2$, 0.05% BSA, and 1 μg/mL (w/v) yeast tRNA]. For selections against Nb-$G_{i\alpha1}$ in the GDP-AlF_4^- state, the selection buffer was supplemented with 10 mM NaF and 25 μM $AlCl_3$. For the selection against Nb-$G_{i\alpha1}$-GDP, stringency was increased in the 4th round by performing the binding at 37 °C and in the 5th and 6th rounds by allowing the target matrix to incubate in selection buffer containing free, non-biotinylated $G_{i\alpha1}$. Selected fusions were PCR amplified for use as the template in the subsequent round and for cloning and DNA sequencing.

Purified RNA-peptide fusions of individual clones were assayed for binding to Nb-$G_{i\alpha1}$ in selection buffer without yeast tRNA. ^{35}S-methionine-labeled fusions were RNase-treated (RNase, DNase-free, Roche) prior to addition to 1 mL of buffer containing ~10 μL of Nb-$G_{i\alpha1}$ (~10 μg) on NeutrAvidin-agarose. After binding at 4 °C for 1 h, 3 × 0.6 mL buffer washes were performed using spin filters (0.45 μm, Costar Spin-X) and the agarose was scintillation counted.

Results

R6A-1 is a core motif for G_α-binding

To investigate the specificity of the R6A-1 minimal peptide, a pull-down assay was developed using radiolabeled, *in vitro* translated G protein subunits (Figure 1A). Cell-free coupled transcription/translation offered a rapid way of screening multiple G proteins (*14-16*) and cDNA clones for human G proteins were readily available. R6A-1 and L19 GPR peptides were synthesized with a C-terminal biotin-containing linker peptide derived from the constant region used in the original selection (*11*). The full-length R6A peptide was also expressed as an N-terminal fusion to MBP, which was subsequently immobilized by random amine coupling. ^{35}S-methionine-labeled $G_{i\alpha1}$ was first tested against immobilized L19 GPR and full-length R6A, demonstrating specific pull-down of full-length $G_{i\alpha1}$, as well as a slightly lower molecular weight band that corresponds to an alternate translation initiation site (Figure 1B).

Previous results demonstrated that the consensus GPR peptide had high affinity for $G_{i\alpha}$ and weaker affinity for $G_{o\alpha}$ (*17, 18*). In our assay, the L19 GPR peptide exhibited binding only to $G_{i\alpha1-3}$ (Figure 2A). The R6A-1 minimal peptide exhibited strong binding for all heterotrimeric G_α subunits tested (Figure 2B). The full-length R6A sequence, however, demonstrated significantly weaker binding to a number of G proteins, especially to G_α o, s, and 15 (Figure 2C). It is not clear whether the differences in affinity to the various G proteins are due to the N-terminal flanking region of the full-length R6A sequence, the altered immobilization scheme (random amine coupling versus C-terminal biotinylation on the R6A-1 peptide), or steric effects from the comparatively

large MBP fusion. However, assuming that the various G proteins are structurally homologous and that the R6A peptide binds to each G_α subunit in the same manner, the differences in relative binding would seem to be a direct result of the R6A flanking residues.

Core motif remains specific for the GDP state

To confirm the interaction of the R6A-derived peptides to various G proteins and establish the nucleotide state specificity, the effect of aluminum fluoride on binding was determined. Previously, it was shown that R6A was highly specific for the GDP state of $G_{i\alpha1}$ and did not bind to either $G_{i\alpha1}$-GDP-AlF_4^- or $G_{i\alpha1}$-GTPγS (*11*). *In vitro* translated, radiolabeled G proteins were assayed for binding to immobilized R6A-1 and R6A-MBP in the presence and absence of aluminum fluoride. The minimal peptide was specific for the GDP state for all G proteins except for G_α 12 and 15, where the effect of aluminum fluoride was negligible (Figure 3A). Full-length R6A-MBP demonstrated strong specificity for the GDP state for all G proteins (Figure 3B), including $G_{12\alpha}$, where aluminum fluoride reduced binding to the background levels seen previously (Figure 2C). The minimal interaction seen with $G_{s\alpha}$ to R6A-MBP was also confirmed, based on the reduced binding in the presence of aluminum fluoride.

R6A competes with $G_{\beta\gamma}$ for binding to G_α subunits

Previously, GPR- and R6A-derived peptides had been shown to compete with $G_{\beta\gamma}$ heterodimers for binding to $G_{i\alpha1}$ (*11, 19-22*). To determine whether R6A would exclude $G_{\beta\gamma}$-binding for other G_α subunits, *in vitro* translated $G_{\beta1}$ and HA-tagged $G_{\gamma2}$ (Figure 4A)

were reconstituted with various G_α subunits and pulled down by immobilized L19 GPR, R6A-MBP, or an anti-HA monoclonal antibody. The tested G_α subunits (i1–3 and q) all appeared to couple to $G_{\beta\gamma}$ heterodimers (Figure 4B). Co-precipitation of G_γ subunits was not seen when heterotrimers were pulled down by L19 GPR or R6A-MBP (Figure 4B), clearly indicating that binding to these motifs excludes $G_{\beta\gamma}$ interaction (Figure 4C). Results for R6A-MBP with reconstituted $G_{12\alpha\beta1\gamma2}$ heterotrimers were similar (data not shown). While the GPR and R6A peptides recognize N-terminal truncations of $G_{i\alpha1-3}$, coupling to $G_{\beta\gamma}$ appears to require the full-length protein (Figure 4B, HA immunoprecipitation).

Peptide competition with $G_{\beta\gamma}$ heterodimers was also demonstrated in a reverse experiment with immobilized G_α subunits. N-terminal biotinylated $G_{i\alpha1-3}$ were immobilized on streptavidin and used to pull-down radiolabeled $G_{\beta\gamma}$. Immobilized G proteins were active for binding $G_{\beta\gamma}$, specifically in the GDP state (Figure 5A). Pull-down assays with single G_β or G_γ subunits on Nb-$G_{i\alpha1}$ resulted in ~10% and ~1% background binding, respectively, compared with reconstituted $G_{\beta\gamma}$-binding (data not shown). It is unclear whether this reflects non-specific binding to the matrix or the presence of free, unlabeled G proteins in the reticulocyte lysate, which would allow formation of intact heterodimers.

Competition with $G_{\beta\gamma}$ was measured by preincubation of immobilized $G_{i\alpha}$ with various concentrations of peptide. Surprisingly, $G_{\beta\gamma}$ competition could not be measured in this assay for the L19 GPR consensus peptide with $G_{i\alpha1}$ (Figure 5B). R6A-1 and full-length R6A-4 peptides demonstrated IC_{50} values of 3.0 and 1.0 μM, respectively, for

$G_{i\alpha1}$. L19 GPR and R6A-4 demonstrated similar IC_{50} values for immobilized $G_{i\alpha3}$ (Figure 5C). The differences in peptide competition for G_α i1 and i3 may result from variations in heterodimer coupling to or peptide recognition of the two G protein subclasses. The negative control peptide C-GPR had no effect on $G_{\beta\gamma}$-coupling for either G_α subunit at concentrations up to 10 μM (data not shown).

mRNA display with a doped R6A-1 library

While the R6A-1 9-mer demonstrated ubiquitous binding to the various G_α subunits, additional flanking residues may confer unique specificities and/or activities to the core peptide. A new mRNA display peptide library was designed and synthesized based on the R6A-1 core motif. The 115.1 template, after PCR amplification, contained a T7 promoter for transcription, an untranslated region (5' UTR), a start codon, the library X_6-DQLYWWEYL-X_6 where the core residues were doped to give approximately 50% wild-type at each R6A-1 residue, and a 3' constant sequence. Sequencing of randomly chosen clones from the initial pool revealed a reasonable distribution for wild-type residues in the core motif, in agreement with theoretical calculations (data not shown).

To demonstrate the utility of the 115.1 core motif library for identifying G protein ligands, *in vitro* selection was performed against immobilized $G_{i\alpha1}$ in the GDP and GDP-aluminum fluoride states. Addition of aluminum fluoride produces a stable $G_{i\alpha1}$-GDP-AlF_4^- complex which mimics the transition state for GTP hydrolysis (*23, 24*). Based on quantitation of the purified, ^{35}S-labeled RNA-peptide fusions and the estimated overall L-methionine concentration, the complexity of the starting library for each selection target was ~2×10^{13}. Selection was performed on immobilized Nb-$G_{i\alpha1}$ due to the previous

finding that the R6A- and GPR-derived peptides bound preferentially to Nb-$G_{i\alpha1}$ over the C-terminal biotinylated Cb-$G_{i\alpha1}$ (*11*). Six rounds of selection were performed against each target, with significant binding observed by the third rounds (Figure 6A and D). Sequences isolated from the selection are listed in Table I.

Alignment of the sequences from the $G_{i\alpha1}$-GDP selection confirmed the original R6A consensus (*11*), although Phe was preferred in the penultimate residue rather than Tyr (Figure 6B). Flanking residues in the random hexamer regions appeared to play a minimal role with no obvious sequence conservation. Positions 17 and 18, however, did seem to favor a Glu-Leu pair. There also seemed to be a preference for positively charged side chains in the N-terminal region, with significantly fewer Lys and Arg residues in the C-terminus (Figure 6C). A reduction in Ala, Ile, Val, and Glu and an increase in Lys, Pro, and Cys were observed when comparing the amino acid usage of the random domains between the 3rd and 6th round sequences. The increase in Cys may improve peptide affinity for the higher stringency selection rounds due to peptide cyclization, oligomerization, or disulfide-bridging with available surface Cys on $G_{i\alpha1}$ during the binding and wash steps. How the peptide properties changed with the shift in usage of other amino acids is unclear.

Selected peptides from the $G_{i\alpha1}$-GDP-AlF_4^- selection (Table II) demonstrated a slightly different consensus than sequences from the GDP state selection (Figure 6E and F). These differences may be critical residues in nucleotide state-specific recognition. Binding assays of several individual sequences, however, reveal only a marginal shift in propensities toward the aluminum fluoride state, with most peptides still favoring the GDP- over the GDP-AlF_4^--bound state. Nevertheless, peptides selected against GDP

(from the C-GPR X6 (*11*) or core motif libraries) clearly demonstrate different binding tendencies than the sequences isolated from the $G_{i\alpha1}$-GDP-AlF_4^- selection (Figure 7).

Discussion

Previously, *in vitro* selection with an mRNA display library was used to isolate novel peptide sequences that act as GDIs for $G_{i\alpha1}$ (*11*). The minimal 9-mer peptide, R6A-1, retained high affinity and competed with $G_{\beta\gamma}$ for binding to $G_{i\alpha1}$. Here, we have further characterized the R6A-derived peptides and have determined that the core motif binds to a variety of G_α subunits representing all four G protein classes. Binding appeared to be specific for heterotrimeric G proteins as there was negligible interaction with the small G protein, H-Ras. Impressively, R6A remained competitive with $G_{\beta\gamma}$ heterodimers for binding to G_α i1–3, q, and 12 (others were untested).

Full-length R6A and the R6A-1 core motif exhibited differences in state specificity and in relative binding to the various G proteins. These findings suggest that flanking residues may play a strong role in modulating the properties of the 9-mer core peptide. The use of flanking residues to gain G protein subclass specificity was recently demonstrated for a GoLoco or GPR peptide derived from RGS14. From the crystal structure of the $G_{i\alpha1}$:GoLoco peptide complex, it was determined that residues C-terminal to the GoLoco consensus, a region that is poorly conserved among GoLoco/GPR-containing proteins, interacted extensively with residues that differed between $G_{i\alpha1}$ and $G_{o\alpha}$ subunits, thereby controlling the specificity of GoLoco-G_α interactions (*25*).

The core motif library was designed to encode the R6A-1 peptide flanked by random hexamers. Nucleotide incorporation was controlled such that approximately 50%

conservation was seen for each "wild-type" residue in the core. This library will be useful for the selection of peptides that are specific for various G protein subclasses or nucleotide-bound states. As a demonstration of the utility of this library, *in vitro* selection was performed against immobilized $G_{i\alpha1}$ in two unique, nucleotide-bound states. $G_{i\alpha1}$-binding peptides were enriched remarkably quickly, as significant binding of the pool was seen in the 3rd selection rounds (Figure 6A and D). Assuming a maximum enrichment of 10- to 1000-fold per round, an estimated 10^7 to 10^{11} unique, $G_{i\alpha1}$-binding peptide sequences were present in the 3rd round pools. Many of these sequences may have unique functions, such as specificity for $G_{i\alpha1}$ over other G_α subunits, which have not yet been identified. We are currently assaying individual clones using a G_α-binding screen to obtain a general gauge of each peptide's properties.

We have previously used a naïve, random 27-mer library to target the $G_{i\alpha1}$-GDP-AlF_4^- state.[2] After eight rounds of selection, enrichment for functional peptides was not seen. The successful selection of peptides against $G_{i\alpha1}$-GDP-AlF_4^- clearly demonstrates the utility of the core motif library in rapidly generating G protein ligands. The $G_{i\alpha1}$-GDP-AlF_4^- complex mimics the transition state for GTP hydrolysis (*23, 24*). RGS proteins, which bind strongly to $G_{i\alpha1}$-GDP-AlF_4^-, act as GAPs, potently catalyzing GTP hydrolysis (*23, 24, 26, 27*). Whether the selected peptides can accelerate GTP hydrolysis for $G_{i\alpha1}$ is under investigation.

We have demonstrated that the core motif library, based on the R6A-1 peptide, is useful for the rapid isolation of G protein-binding peptides. The structural determination

[2] Ja and Roberts, unpublished results.

of an R6A-derived peptide:$G_{i\alpha 1}$ complex will greatly facilitate the molecular design of other specific, potent modulators of G protein signaling. The Ras family of small G proteins represents another rich source of bona fide drug targets (*28-30*). Whether the core motif library can be used against this G protein superfamily, which shares significant structural homology to the nucleotide-binding (Ras-like) domain of heterotrimeric G_α subunits, is unknown. Future directions include using the library to target other heterotrimeric G protein classes and nucleotide-bound states (e.g., G_α-GTP or nucleotide-free). The use of free, non-immobilized G protein competitors will enable the direct selection of peptides that are specific for particular G_α subclasses.

Acknowledgments

We are grateful for suggestions on G protein translation provided by Dr. Bradley M. Denker (Harvard Institutes of Medicine) and Prof. Carl Schmidt (University of Delaware). Dr. David S. Waugh (National Cancer Institute at Frederick) generously provided the original pDW363 vector. We also thank Dr. Yuri K. Peterson (Duke University) for advice on characterizing the R6A-derived peptides and Terry T. Takahashi and Christine T. Ueda for comments on the manuscript. This work was supported by grants from the NIH (RO160416) and the Beckman Foundation to R. W. R. W. W. J. was supported in part by a DOD National Defense Science and Engineering Graduate Fellowship. R. W. R. is an Alfred P. Sloan Foundation Research Fellow.

References

1. Gilman, A. G. (1987) G proteins: transducers of receptor-generated signals, *Annu. Rev. Biochem. 56*, 615-649.
2. Neves, S. R., Ram, P. T., and Iyengar, R. (2002) G protein pathways, *Science 296*, 1636-1639.
3. Drews, J. (2000) Drug discovery: a historical perspective, *Science 287*, 1960-1964.
4. Howard, A. D., McAllister, G., Feighner, S. D., Liu, Q., Nargund, R. P., Van der Ploeg, L. H., and Patchett, A. A. (2001) Orphan G-protein-coupled receptors and natural ligand discovery, *Trends Pharmacol. Sci. 22*, 132-140.
5. Höller, C., Freissmuth, M., and Nanoff, C. (1999) G proteins as drug targets, *Cell. Mol. Life Sci. 55*, 257-270.
6. Nürnberg, B., Tögel, W., Krause, G., Storm, R., Breitweg-Lehmann, E., and Schunack, W. (1999) Non-peptide G-protein activators as promising tools in cell biology and potential drug leads, *Eur. J. Med. Chem. 34*, 5-30.
7. Radhika, V., and Dhanasekaran, N. (2001) Transforming G proteins, *Oncogene 20*, 1607-1614.
8. Spiegel, A. M., and Weinstein, L. S. (2004) Inherited diseases involving G proteins and G protein-coupled receptors, *Annu. Rev. Med. 55*, 27-39.
9. Dower, W. J., and Mattheakis, L. C. (2002) *In vitro* selection as a powerful tool for the applied evolution of proteins and peptides, *Curr. Opin. Chem. Biol. 6*, 390-398.

10. Lin, H., and Cornish, V. W. (2002) Screening and selection methods for large-scale analysis of protein function, *Angew. Chem. Int. Edit. 41*, 4402-4425.

11. Ja, W. W., and Roberts, R. W. (2004) *In vitro* selection of state-specific peptide modulators of G protein signaling using mRNA display, *Biochemistry 43*, 9265-9275.

12. Tsao, K.-L., DeBarbieri, B., Michel, H., and Waugh, D. S. (1996) A versatile plasmid expression vector for the production of biotinylated proteins by site-specific, enzymatic modification in *Escherichia coli*, *Gene 169*, 59-64.

13. Neer, E. J., Denker, B. M., Thomas, T. C., and Schmidt, C. J. (1994) Analysis of G-protein α and βγ subunits by *in vitro* translation, *Methods Enzymol. 237*, 226-239.

14. Garcia-Higuera, I., Thomas, T. C., Yi, F., and Neer, E. J. (1996) Intersubunit surfaces in G protein αβγ heterotrimers. Analysis by cross-linking and mutagenesis of βγ, *J. Biol. Chem. 271*, 528-535.

15. Mende, U., Schmidt, C. J., Yi, F., Spring, D. J., and Neer, E. J. (1995) The G protein γ subunit. Requirements for dimerization with β subunits, *J. Biol. Chem. 270*, 15892-15898.

16. Schmidt, C. J., and Neer, E. J. (1991) *In vitro* synthesis of G protein βγ dimers, *J. Biol. Chem. 266*, 4538-4544.

17. Peterson, Y. K., Bernard, M. L., Ma, H., Hazard, S., III, Graber, S. G., and Lanier, S. M. (2000) Stabilization of the GDP-bound conformation of Giα by a peptide

derived from the G-protein regulatory motif of AGS3, *J. Biol. Chem. 275*, 33193-33196.

18. Peterson, Y. K., Hazard, S., III, Graber, S. G., and Lanier, S. M. (2002) Identification of structural features in the G-protein regulatory motif required for regulation of heterotrimeric G-proteins, *J. Biol. Chem. 277*, 6767-6770.

19. Bernard, M. L., Peterson, Y. K., Chung, P., Jourdan, J., and Lanier, S. M. (2001) Selective interaction of AGS3 with G-proteins and the influence of AGS3 on the activation state of G-proteins, *J. Biol. Chem. 276*, 1585-1593.

20. Natochin, M., Gasimov, K. G., and Artemyev, N. O. (2001) Inhibition of GDP/GTP exchange on Gα subunits by proteins containing G-protein regulatory motifs, *Biochemistry 40*, 5322-5328.

21. Natochin, M., Lester, B., Peterson, Y. K., Bernard, M. L., Lanier, S. M., and Artemyev, N. O. (2000) AGS3 inhibits GDP dissociation from Gα subunits of the G_i family and rhodopsin-dependent activation of transducin, *J. Biol. Chem. 275*, 40981-40985.

22. De Vries, L., Fischer, T., Tronchère, H., Brothers, G. M., Strockbine, B., Siderovski, D. P., and Farquhar, M. G. (2000) Activator of G protein signaling 3 is a guanine dissociation inhibitor for $G\alpha_i$ subunits, *Proc. Natl. Acad. Sci. U.S.A. 97*, 14364-14369.

23. Berman, D. M., Kozasa, T., and Gilman, A. G. (1996) The GTPase-activating protein RGS4 stabilizes the transition state for nucleotide hydrolysis, *J. Biol. Chem. 271*, 27209-27212.

24. Tesmer, J. J. G., Berman, D. M., Gilman, A. G., and Sprang, S. R. (1997) Structure of RGS4 bound to AlF_4^--activated $G_{i\alpha1}$: Stabilization of the transition state for GTP hydrolysis, *Cell 89*, 251-261.

25. Kimple, R. J., Kimple, M. E., Betts, L., Sondek, J., and Siderovski, D. P. (2002) Structural determinants for GoLoco-induced inhibition of nucleotide release by Gα subunits, *Nature 416*, 878-881.

26. Berman, D. M., Wilkie, T. M., and Gilman, A. G. (1996) GAIP and RGS4 are GTPase-activating proteins for the G_i subfamily of G protein α subunits, *Cell 86*, 445-452.

27. Srinivasa, S. P., Watson, N., Overton, M. C., and Blumer, K. J. (1998) Mechanism of RGS4, a GTPase-activating protein for G protein α subunits, *J. Biol. Chem. 273*, 1529-1533.

28. Barbacid, M. (1987) *ras* genes, *Annu. Rev. Biochem. 56*, 779-827.

29. Bos, J. L. (1989) *ras* oncogenes in human cancer: a review, *Cancer Res. 49*, 4682-4689.

30. Malumbres, M., and Barbacid, M. (2003) *RAS* oncogenes: the first 30 years, *Nat. Rev. Cancer 3*, 459-465.

31. Schneider, T. D., and Stephens, R. M. (1990) Sequence logos: a new way to display consensus sequences, *Nucleic Acids Res. 18*, 6097-6100.

32. Crooks, G. E., Hon, G., Chandonia, J. M., and Brenner, S. E. (2004) WebLogo: a sequence logo generator, *Genome Res. 14*, 1188-1190.

Tables

Table I. Sequences of peptides selected against $G_{i\alpha 1}$-GDP.[a]

	Clone	Peptide sequence
Library	115.1	**XXXXXX *DQLYWWEYL* XXXXXX** GGYTSLSA
Round 3	R3-01	**MINTGD DELYWWQFL AELPVL** GGYTSLSA
	R3-02	**ASVHFT DKLHWWEFL EMSRDI** GGYTSLSA
	R3-03	**LEISGL DQVYWWEFL NELLSE** GGYTSLSA
	R3-04	**RLEMAS DKIYWWEYL AELASV** GGYTSLSA
Round 4	R4-01	**RDNMNR DELYWWEFL LEAVSE** GGYTSLSA
	R4-02	**ITIGAD DQLYWWEFL SDFHPQ** GGYTSLSA
	R4-03	**KEMWMD DQLYWWEFV LDTPLL** GGYTSLSA
	R4-04	**KRCNLT DELYWWEYL QSPHVA** GGYTSLSA
	R4-05	**NDWEST HRLYWWEFL EGMSTS DGYTSLSA**
	R4-07	**MMDSSN DQIYWWEFL DSWPLK** GGYTSLSA
	R4-08	**HTKLGN AKLSLEEFL LWLNDS** GGYTSLSA
Round 5	R5-01	**MHWHNT YQLSWWEFL DELDYN** GGYTSLSA
	R5-02	**DKENWH DQLYWWEFL ADYTNG** GGYTSLSA
	R5-03	**EESSLM DLMHWWEFL SELDCA** GGYTSLSA
	R5-04	**GSLNQW DRLYWWEFL ALCDSA** GGYTSLSA
	R5-05	**IESRLQ DLVYWWEAL LPTDSG** GGYTSLSA
	R5-06	**KGVSKR DQMTWWEFL SSPTGE** GGYTSLSA
	R5-07	**MLNCDN DKIYWWEYL REAPEA** GGYTSLSA
Round 6	R6-01	**KTNFWT AELNLCEFL CELDEL** GGYTSLSA
	R6-02	**HGLSMR DKLYWWEFL LDSTPN** GGYTSLSA
	R6-03	**TKCSLN DRVYWWEFL QCNSQK** CGYTSLSA
	R6-04	**TMNSLC DQLFWWEFL AQTSNL** DGYTSLSA
	R6-05	**KKPHER ESCCGRTGC RPCRSS AVTLVCL**
	R6-06	**LLTDLA AQLYWWEFL DMESGS** DGYTSLSA
	R6-07	**MENFWM DQLYWWEFI MELHDL** GGYTSLSA
	R6-08	**RTCNPD DLIYWWEYL SCPSCE** GGYTSLSA

[a] Sequences are in bold except for the C-terminal constant region. The 9-mer core (in italics) of the 115.1 core motif library was encoded by the DNA template to be conserved approximately 50% "wild-type" at each position. Clones R4-05, R6-03, R6-04, and R6-06 contained point mutations in the constant region, while clone R6-05 had a deletion resulting in a frame-shift. Except for the C-terminal constant sequence, residues are colored by amino acid type (red, positively charged; blue, negatively charged; black, polar; gray, non-polar). The methionine start codon is not shown.

Table II. Sequences of peptides selected against $G_{i\alpha 1}$-GDP-AlF_4^-.[a]

	Clone	Peptide sequence
Library	115.1	XXXXXX *DQLYWWEYL* XXXXXX GGYTSLSA
Round 6	R6-02	GSASDT DLMYWWEFL REPNRG GGYTSLSA
	R6-04	TKLRMT DNLGWGFLI LPSQF GGYTSLSA
	R6-05	DESDPE ELMYWWEFL SEDPSS GGYTSLSA
	R6-06	AHAKNL DLLTWWEFL SETNST GGYTSLSA
	R6-07	KLGNES DLLYWWEFL DQNEDD GGYTSLSA
	R6-09	KRHKLT DQLYWWEFL RDSYDD GGYTSLSA
	R6-11	EMRNQN ALLYWWEYL DELARS DGYTSLSA
	R6-12	MTSWLD DQLYWWEYL DECSRA GGYTSLSA
	R6-13	NMDRLN DLLYWWEFL EDEAPH GGYTSLSA
	R6-14	ITTMDD ELLYWWEYL DSLPQL GGYTSLSA
	R6-17	RKTHLS DLVYWWEFL AEDEDD GGYTSLSA
	R6-18	YWVDRY DERSGVCLG RQKNR GGYTSLSA
	R6-19	KLNFTN DELDWWESL MLALTT SGYTSLSA
	R6-20	YMDDND DLVYWWEFL LEPFPS GGYTSLSA
	R6-21	ALRLDV EPRNGWGFV LNPYNL GGYTSLSA
	R6-22	SDEYLD EKLYWWDFL SQMNDL GGYTSLSA
	R6-23	HKMMGS DLIYWWEFL DEINNE GGYTSLSA

[a] Sequences are shown as in Table I. Clones R6-04 and R6-18 had 3 bp deletions, while clones R6-11 and R6-19 contained point mutations in the constant region. All sequences were from the 6th round of selection.

Figures

Figure 1. Binding analysis with *in vitro* translated G proteins. (A) The indicated G_{α} subunits or H-Ras were directly translated from human cDNA vectors in a coupled transcription/translation reaction with ^{35}S-methionine labeling. A blank reaction (−) did not contain vector. The slightly lower molecular weight bands (seen clearly for $G_{i\alpha1}$ and $G_{i\alpha3}$) correspond to translation initiation at alternate methionine codons. (B) Pull-down of radiolabeled $G_{i\alpha1}$ on full-length R6A-MBP or L19 GPR peptide. R6A-MBP (+) was immobilized on cyanogen bromide-activated sepharose, while the negative control (−) contained MBP only. The L19 GPR peptide was immobilized on streptavidin-agarose, using the matrix without peptide as a negative control (−).

Figure 2. Binding of various *in vitro* translated G proteins to (A) L19 GPR, (B) R6A-1, and (C) R6A-MBP. Binding is shown relative to the estimated protein translation efficiency, as determined by TCA precipitation (see methods). The negative control matrices used in the assay were (A and B) streptavidin-agarose and (C) immobilized MBP-sepharose. $G_{12\alpha}$ consistently exhibited high non-specific binding which was especially noticeable on the MBP-sepharose in (C).

Figure 3. Binding of various *in vitro* translated G proteins to (A) R6A-1 and (B) R6A-MBP in the presence and absence of aluminum fluoride. R6A-MBP was highly specific to the GDP state while the minimal peptide, R6A-1, was GDP state specific only for G_{α} i1–3, oA, q, and s(s). Binding of $G_{12\alpha}$ to R6A-MBP in the presence of aluminum fluoride

was approximately equal to the non-specific binding seen previously (compare with Figure 2C).

Figure 4. R6A-MBP and L19 GPR compete with $G_{\beta\gamma}$ for binding to G_{α} subunits. (A) *In vitro* translated $G_{\beta 1}$ and HA-tagged $G_{\gamma 2}$ subunits. (B) Reconstituted $G_{\alpha\beta\gamma}$ heterotrimers (with G_{α} i1–3 or q) were pulled down with an anti-HA antibody, R6A-MBP, or L19 GPR. Only the G_{α} and $G_{\gamma 2}$ subunits were radiolabeled. Immunoprecipitation with anti-HA confirmed the presence of reconstituted heterotrimers in the reaction mix. G_{γ} was not co-precipitated when G_{α} subunits were pulled down by R6A-MBP or L19 GPR. Results were similar for $G_{12\alpha}$ (data not shown). (C) Binding of G_{α}-GDP to $G_{\beta\gamma}$ and R6A appear to be exclusive events.

Figure 5. R6A and GPR peptides compete with $G_{\beta\gamma}$ for binding to $G_{i\alpha}$ subunits. (A) Binding of radiolabeled $G_{\beta\gamma}$ to immobilized $G_{i\alpha 1-3}$ in the presence and absence of aluminum fluoride. The negative control (−) represents binding of $G_{\beta\gamma}$ to the matrix without immobilized G_{α}. IC_{50} values for peptide competition with $G_{\beta\gamma}$ heterodimers were determined for (B) $G_{i\alpha 1}$ and (C) $G_{i\alpha 3}$ by preincubating immobilized G_{α} with increasing concentrations of peptide prior to the binding assay. For the competition studies, binding limits have been scaled relative to the amount of $G_{\beta\gamma}$ bound in the absence of peptide (± aluminum fluoride for the lower and upper bounds, respectively). Sigmoidal fits were performed with Origin 6.0 Professional (OriginLab Corp., Northampton, MA) with the lower bound fixed at zero.

Figure 6. Selection of the 115.1 core motif library against $G_{i\alpha1}$ in the (A-C) GDP- and (D-F) GDP-AlF_4^--bound states. (A and D) Binding of RNA-peptide fusions from each round of selection. In rounds 4, 5, and 6 of the $G_{i\alpha1}$-GDP selection, stringency was increased by performing the binding at higher temperature or by adding free $G_{i\alpha1}$ as a competitor. (B and E) Sequence logo (*31*) representations of all sequences recovered from the selections (Tables I and II), generated using WebLogo (*32*) at http://weblogo.berkeley.edu. Only the X_6-R6A-1-X_6 region is shown. Residues are colored according to amino acid type: black, polar [CHNQSTWY]; gray, non-polar [AFGILMPV]; blue, negatively charged [DE]; and red, positively charged [KR]. (C and F) Percentage of amino acid types at each position using all sequences recovered from the selection. Color-coding is the same as in B and E.

Figure 7. Binding of individual peptide clones from the C-GPR X6 (*11*) and 115.1 core motif library selections to $G_{i\alpha1}$-GDP or $G_{i\alpha1}$-GDP-AlF_4^-. Purified, RNase-treated RNA-peptide fusions of each clone were assayed for binding against immobilized $G_{i\alpha1}$ in the GDP- or GDP-AlF_4^--bound states. Data are plotted as the fraction of input peptides bound to $G_{i\alpha1}$-GDP (Y-axis) versus $G_{i\alpha1}$-GDP-AlF_4^- (X-axis). While only one of the peptides from the core motif library selection against $G_{i\alpha1}$-GDP-AlF_4^- actually favored the GDP-AlF_4^--state (1.0% versus 0.6% binding for the aluminum fluoride and GDP states, respectively), the binding data from this selection clearly indicate a loss of nucleotide-state preference (toward the black line, which represents 1:1 binding to both states), compared with the other two selections that targeted $G_{i\alpha1}$-GDP. Non-specific

binding to the matrix was generally less than 0.1%. Binding data is tabulated in Supplemental Table I (see Supporting Information).

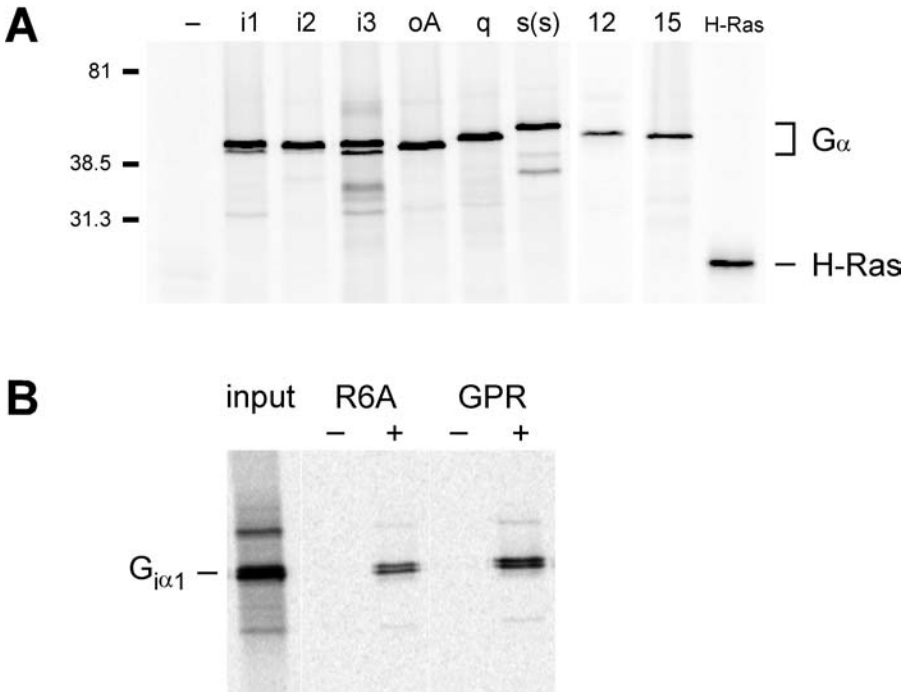
A
–
i1
i2
i3
oA
q
s(s)
12
15
H-Ras
81
38.5
31.3
Gα
H-Ras
B
input
R6A
GPR
–
+
–
+
Gi α1

Figure 1

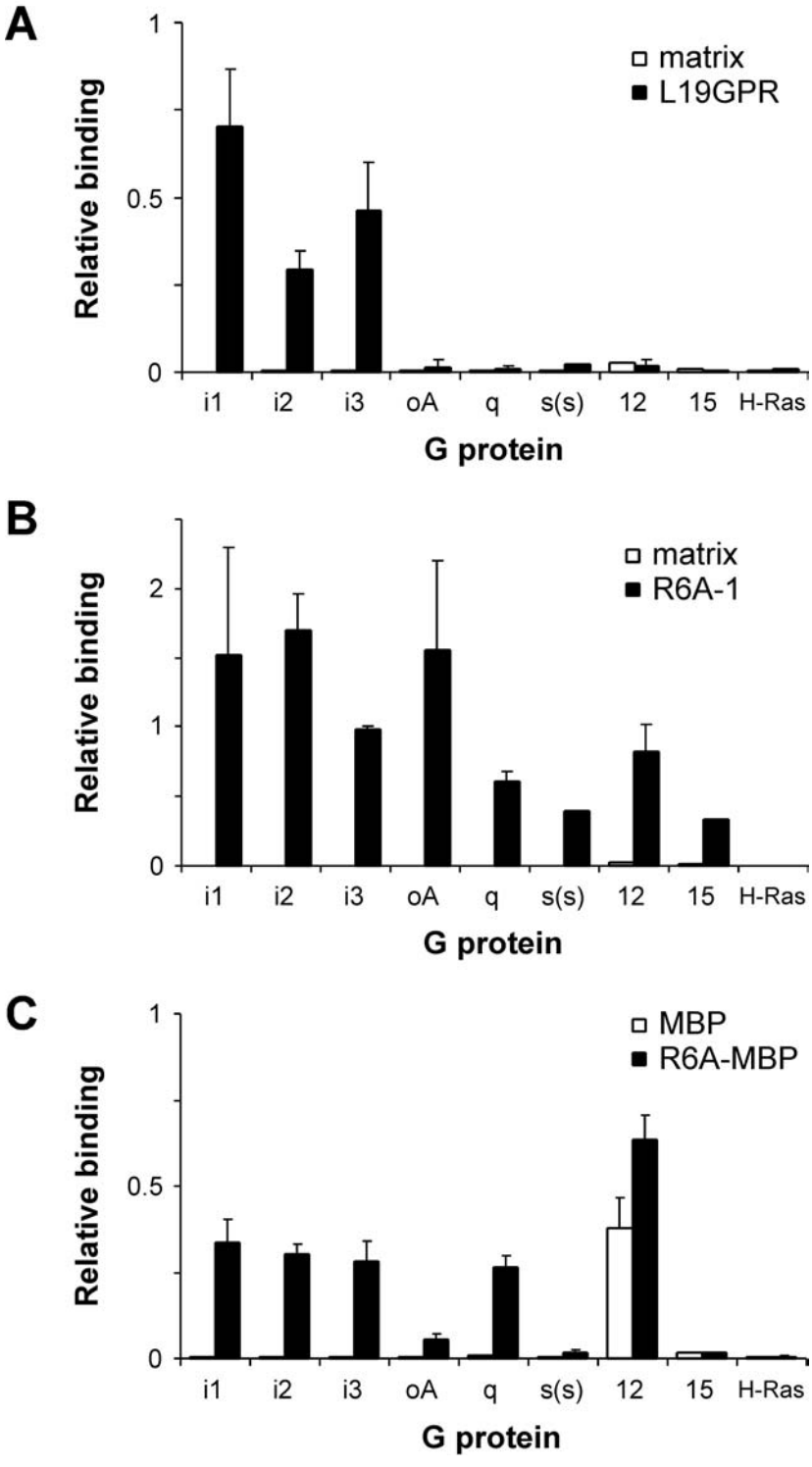
A
Relative binding
1
0.5
0
matrix
L19GPR
i1
i2
i3
oA
q
s(s)
12
15
H-Ras
G protein
B
Relative binding
2
1
0
matrix
R6A-1
i1
i2
i3
oA
q
s(s)
12
15
H-Ras
G protein
C
Relative binding
1
0.5
0
MBP
R6A-MBP
i1
i2
i3
oA
q
s(s)
12
15
H-Ras
G protein

Figure 2

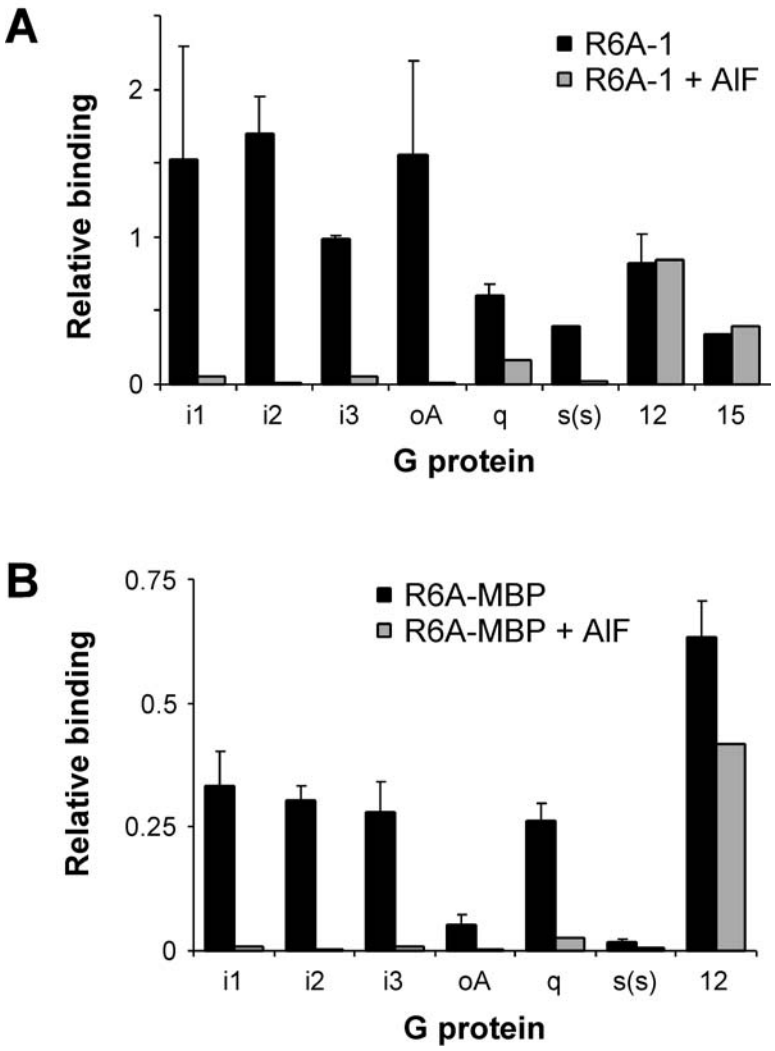
A
R6A-1
R6A-1 + AlF
Relative binding
2
1
0
i1
i2
i3
oA
q
s(s)
12
15
G protein
B
R6A-MBP
R6A-MBP + AlF
Relative binding
0.75
0.5
0.25
0
i1
i2
i3
oA
q
s(s)
12
G protein

Figure 3

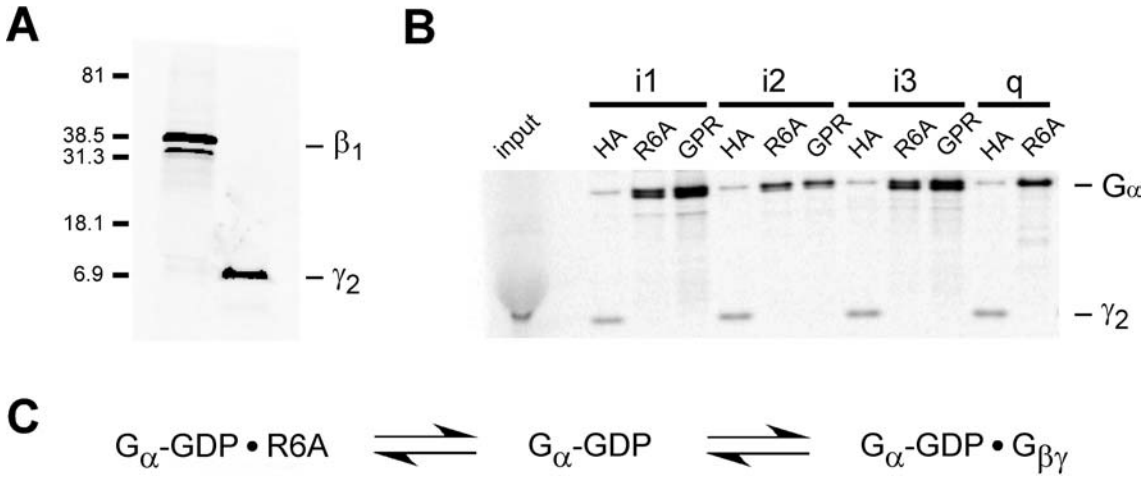
A
81
38.5
31.3
18.1
6.9
– β1
– γ2
B
input
i1
i2
i3
q
HA
R6A
GPR
– Gα
– γ2
C
Gα-GDP • R6A
Gα-GDP
Gα-GDP • Gβγ

Figure 4

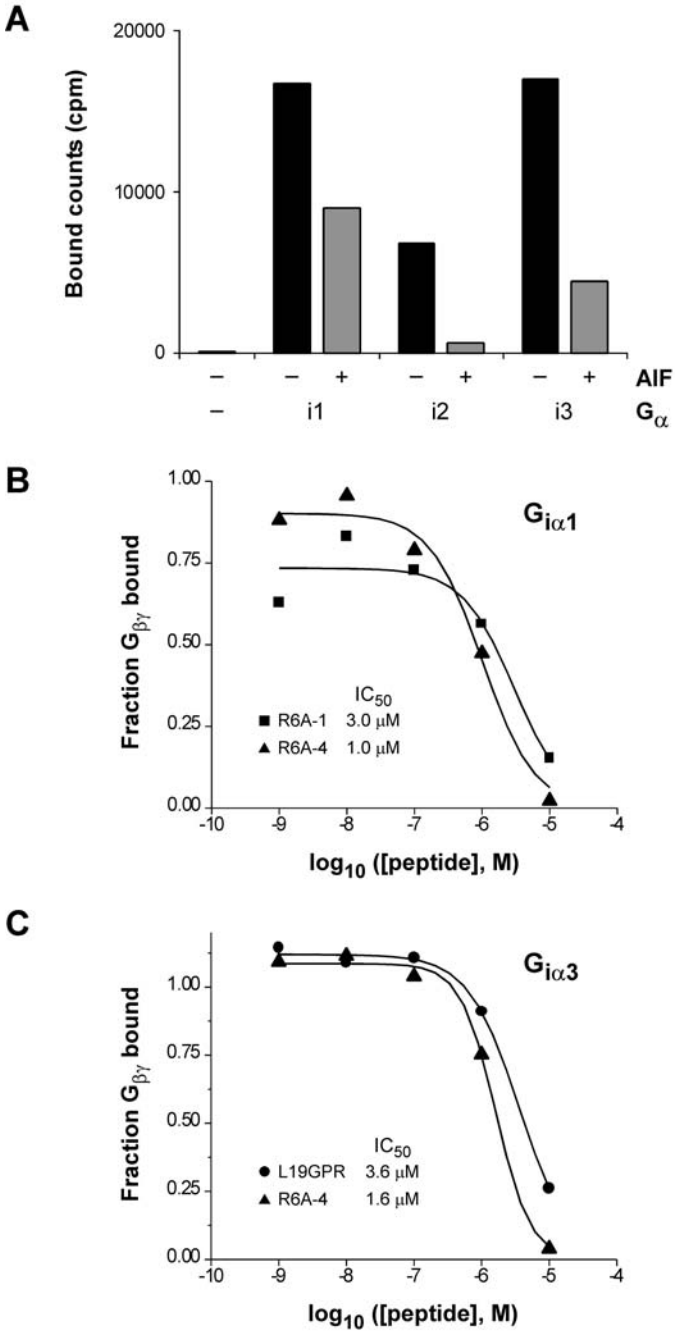
A
Bound counts (cpm)
20000
10000
0
– – + – + – + AlF
– i1 i2 i3 Gα
B
Fraction Gβγ bound
1.00
0.75
0.50
0.25
0.00
Giα1
IC50
R6A-1 3.0 μM
R6A-4 1.0 μM
-10 -9 -8 -7 -6 -5 -4
log10 ([peptide], M)
C
Fraction Gβγ bound
Giα3
IC50
L19GPR 3.6 μM
R6A-4 1.6 μM
log10 ([peptide], M)

Figure 5

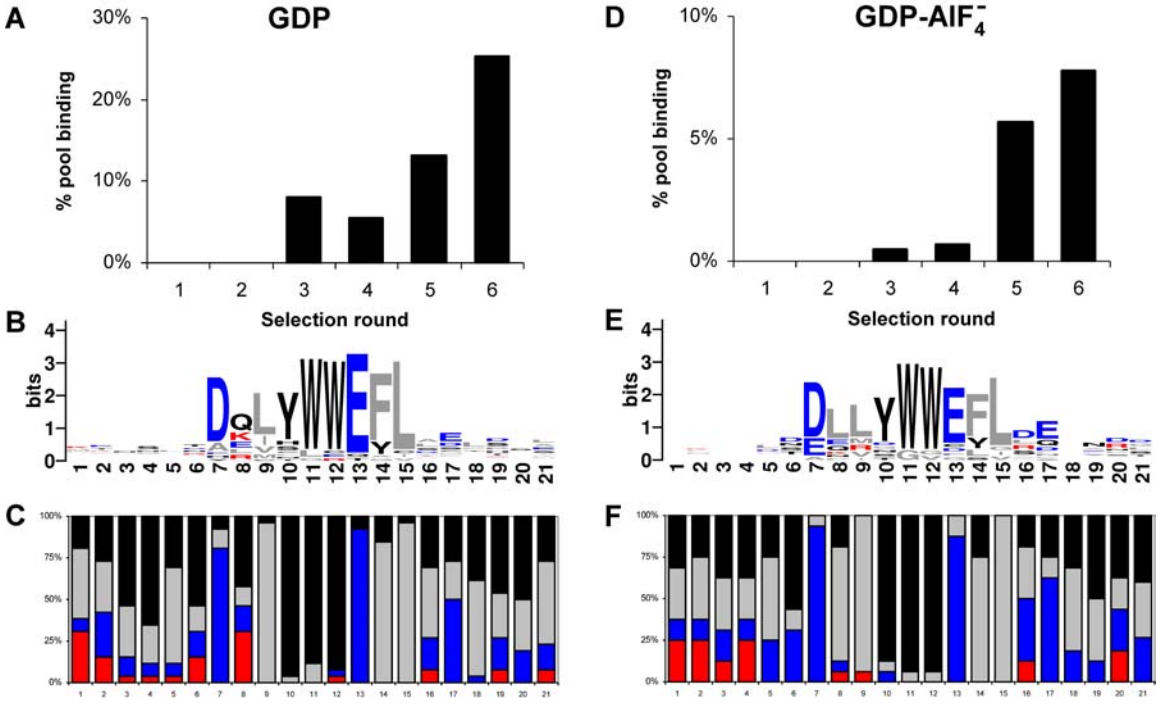
A
GDP
% pool binding
30%
20%
10%
0%
1 2 3 4 5 6
D
GDP-AlF4-
% pool binding
10%
5%
0%
1 2 3 4 5 6
B
Selection round
bits
E
Selection round
bits
C
F

Figure 6

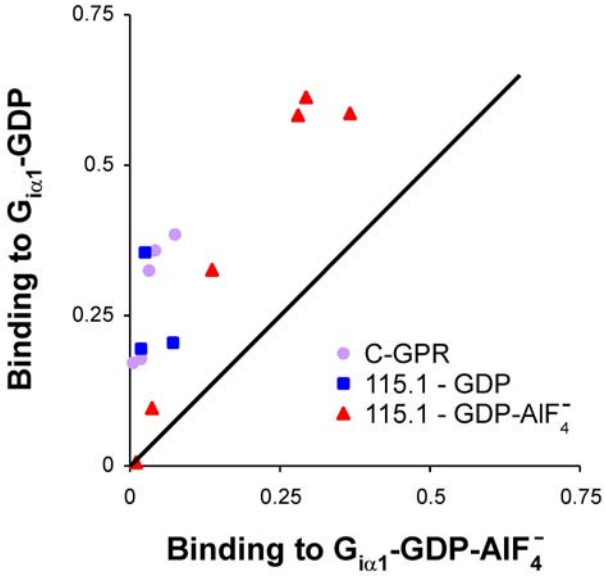
0.75
0.5
0.25
0
0
0.25
0.5
0.75
Binding to $G_{i\alpha1}$-GDP
Binding to $G_{i\alpha1}$-GDP-AlF_4^-
C-GPR
115.1 - GDP
115.1 - GDP-AlF_4^-

Figure 7

Supporting Information

Supplemental Table I. Tabulated binding data for individual peptide clones assayed in Figure 7.

Selection	Peptide [a]	% Binding	
		$G_{i\alpha 1}$-GDP	$G_{i\alpha 1}$-GDP-AlF_4^-
C-GPR X6 GDP	R6A	32.5%	3.4%
	CR7-A	17.0%	0.6%
	CR7-H	17.7%	2.0%
	CR8-B	38.3%	7.7%
	CR8-C	35.6%	4.2%
115.1 GDP	R4-01	20.2%	7.3%
	R4-04	35.3%	2.6%
	R4-05	19.4%	2.0%
115.1 GDP-AlF_4^-	R6-02	61.2%	29.4%
	R6-04	0.6%	1.0%
	R6-05	58.7%	36.6%
	R6-06	32.5%	13.8%
	R6-07	58.3%	28.1%
	R6-08	9.5%	3.7%

[a] Selected peptides from the C-GPR X6 library selection (*11*) are shown in in Supplemental Table II. Peptide sequences from the 115.1 core motif library selections are shown in Tables I and II.

Supplemental Table II. Sequences of peptides from the C-GPR X6 library selection (*11*).

Peptide	Sequence
R6A	MSQTKRLDDQLYWWEYL
CR7-A	MSQSKRLDDQLTWLEFL
CR7-H	MSQSKQLTITEFLQWL
CR8-B	MSQSERLDDQWTWWEFL
CR8-C	MSQSKRLEITWWEFVEQL